IJEMME
INTERNATIONAL JOURNAL of ELECTRONICS, MECHANICAL and MECHATRONICS ENGINEERING

Year: **2019** Volume **9** Number **1**

International Journal of Electronics, Mechanical and Mechatronics Engineering (IJEMME)

PRINTED BY

Armoninuans Matbaa Yukarıdudullu, Bostancı Yolu Cad. Keyap Çarşı B-1 Blk. No:24 Ümraniye/İstanbul
Tel: 0216 540 36 11 Fax: 0216 540 42 72 E-mail: info@armoninuans.com

ISSN: 2146-0604

International Journal of Electronics, Mechanical and Mechatronics Engineering (IJEMME) is peer-reviewed journal which provides a platform for publication of original scientific research and applied practice studies. Positioned as a vehicle for academics and practitioners to share field research, the journal aims to appeal to both researchers and academicians.

Internationally indexed by EBSCO and DOAJ

CONTENTS

From the Editor

International Journal of Electronics, Mechanical and Mechatronics Engineering (IJEMME), is an international multi-disciplinary journal dedicated to disseminate original, high-quality analytical and experimental research articles on Robotics, Mechanics, Electronics, Telecommunications, Control Systems, System Engineering, Biomedical and Renewable Energy Technologies. Contributions are expected to have relevance to an industry, an industrial process, or a device. Subject areas could be as narrow as a specific phenomenon or a device or as broad as a system.

The manuscripts to be published are selected after a peer review process carried out by our board of experts and scientists. Our aim is to establish a publication which will be abstracted and indexed in the Engineering Index (EI) and Science Citation Index (SCI) in the near future. The journal has a short processing period to encourage young scientists.

Prof. Dr. Hasan HEPERKAN
Editor

INTERNATIONAL JOURNAL OF ELECTRONICS, MECHANICAL AND MECHATRONICS ENGINEERING
Vol.9 Num.1 - 2019 (1625-1636)

A Research On Deformation Based Buckling Damage Limit For Reinforced Concrete Columns

Ghulam Mostafa WAZIRY[1], Assoc. Prof. Dr. Cem AYDEMİR[2]

Öz: Elastik ötesi taleple zorlanan betonarme bir kolonunda boyuna donatı burkulma hasarının meydana gelmesi, elemanın taşıma gücünde ani ve belirgin bir azalmaya sebep olur. Son yıllarda yaygın biçimde kullanılmaya başlanan birim şekil değiştirme esaslı tasarım yöntemleriyle, kuvvete dayalı yöntemlere nispeten yapısal hasar daha gerçekçi biçimde belirlenebilmektedir. Bu çalışmada, betonarme yapı elemanlarında birim şekil değiştirme esaslı bir burkulma hasar sınırı tanıtılarak, bu birim şekil değiştirme sınırının deneysel sonuçlar ile karşılaştırması yapılmıştır.

Anahtar Kelimeler: *Hasar sınırı, Burkulma, Burkulma birim şekil değiştirme sınırı, yük-yerdeğiştirme*

A Research On Deformation Based Buckling Damage Limit For Reinforced Concrete Columns

Abstract: Buckling damage at longitudinal reinforcement of a reinforced concrete column under inelastic demand, leads to a rapid and significant decrease in capacity. Structural damage can be obtained in a more realistic way with deformation based design methods compared to force based methods. In this study, an existing deformation based buckling damage limit state is introduced and the comparison of mentioned damage limit state with experimental results is carried out.

Keywords: *Damage limit, buckling, buckling strain limit, load-deflection*

[1] *Istanbul Aydın University, Institute of Science and Technology, Department of Civil Engineering, eng.waziry1697@gmail.com*
[2] *Istanbul Aydın University, Faculty of Engineering, Department of Civil Engineering, cemaydemir@aydin.edu.tr*

1. Introduction

In the case of a ductile reinforced concrete structural element dimensioned according to the capacity design principles, with a reversible cyclical loading to an elastic transverse displacement capacity, the damage observed in the element can be listed as such: cracking in sections, yield in longitudinal reinforcement, crushing in confined concrete, crushing in wound concrete, buckling in longitudinal reinforcement and breakage in longitudinal reinforcement. As the longitudinal reinforcement buckling that may occur after the crushing occurring in the shell concrete under cyclical loading causes a sudden and significant decrease in the load bearing capacity, it can be shown as one of the main damage limits describing the crash damage.

Many behavioral models have been developed based on experimental studies for the behavior of reinforcing steel under monotonic and cyclical loads in reinforced concrete structural elements.**[1~8]** The realism of these behavior models is important for realistic modeling of the seismic performance of the reinforced concrete structural elements.

In this study, an analytical buckling damage limitation based on unit deformation for reinforced concrete structural elements will be introduced. The results of this analytical damage limit approach will be examined comparing with the experimental results of the columns tested by analogy with earthquake loads with constant axial load and reversible cyclic displacement loading.

2. Compression Reinforcement Sprain Deformation Limit

The differentiation of the behavior of reinforced concrete steels under axial tension and pressure has been the subject of many experimental studies. In these studies, which are done on the the samples of the individual rebar samples, that are buckling displacement is shown schematically in Figure 2.1, At the primary level, the effects of the material and loading properties are reported to be affected at the secondary level by the rod free length / diameter ratio (s/□□□of the axial pressure behavior of the reinforcing steel.**[2, 4, 9]**

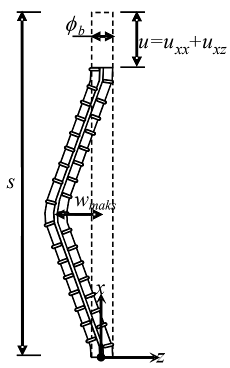

Figure 2.1: Displacement profile of the buckled rebar [10]

Aydemir and Eser [10] conducted investigations for the buckling deformation limit for reinforced concrete rebars under pressure load. In these investigations, by using the results of a comprehensive experimental study under the influence of pressure, [8], the bending unit shortening limit is expressed with the following (1) relation, by considering the effective parameters of the behavior model [8] developed by Bae.**[10]**

$$\frac{s}{\phi_b} \geq 9, \qquad \varepsilon'_{s,L(\%5)} = \varepsilon_{sy} + 0.02 \cdot e^{\left(1.09 \cdot \frac{f_{su}}{f_y} - 0.33 \cdot \frac{s}{\phi_b}\right)}$$
$$6 \leq \frac{s}{\phi_b} < 9, \quad \varepsilon'_{s,L(\%5)} = \varepsilon_{sy} + 0.06 \cdot e^{\left(3.85 \cdot \frac{f_{su}}{f_y} - 0.86 \cdot \frac{s}{\phi_b}\right)} \tag{1}$$

In the relation, $\varepsilon'_{s,L(\%5)}$ denotes the unit deformation limit which corresponds to the condition where the stress reinforcement stress falls to 95% of the yield stress, ε_{sy} denotes the longitudinal reinforcement flow rate change and the ratio of the tensile strength of the reinforcement steel to the yield strength, and s/ϕ_b denotes the ratio of the length of the sprain to the length of the longitudinal reinforcement.

For a reinforced concrete element with weak lateral reinforcement, the buckling length (s) in relation to (1) can be considered equal to the stirrup spacing. On the other hand, longitudinal and transverse reinforcement arrangement may be different in different reinforced concrete sections. For such cases, Aydemir and Eser [10], with the help of an energy based method [11] developed by Dhakal and Maekawa, developed the relation (2) given below for buckling length (s).

$$\zeta = \frac{32 \cdot \frac{A_{sh}}{d_h} \cdot \left(\frac{s_e}{\phi_b}\right)^2 \cdot s_e}{\pi^4 \cdot A_s' \cdot \sqrt{\frac{f_y}{400}}} \tag{2}$$
$$\frac{s}{s_e} = maks\left(1; 0.7 + \frac{0.24}{\zeta}\right)$$

In the relation, A_{sh}, is lateral reinforcement cross-sectional area, s_e is lateral reinforcement range and A_s' is compression reinforcement cross section.

3. Comparing The Experimental Results With The Buckling Unit Deformation Limit

In this section, the boundary deflection limit of buckling damage, which is developed by the behavior of the individual reinforcing bar samples and expressed by (1), will be compared to the results of the reinforced concrete column tests which are forced by analogy with constant axial load and earthquake loading under cyclical horizontal load. The comparisons will be made with the help of the experimental results of 41 column samples tested by various researchers in addition to the column samples produced and tested in Istanbul Aydın University Civil Engineering laboratory.

4. Istanbul Aydın University Experiments

The geometry and reinforcement detail drawings of the test sample produced and tested in Istanbul Aydın University Civil Engineering Laboratory are shown in Figure 3.1 and the test scheme applied in the experimental program is shown schematically in Figure 3.2. The general properties of the test sample are summarized in Table 1.

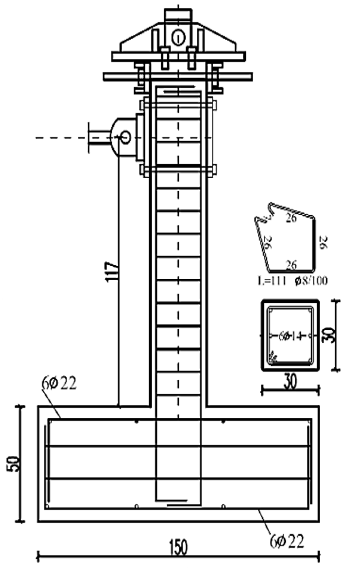

Figure 3.1: Detail of geometry and reinforcement of test sample

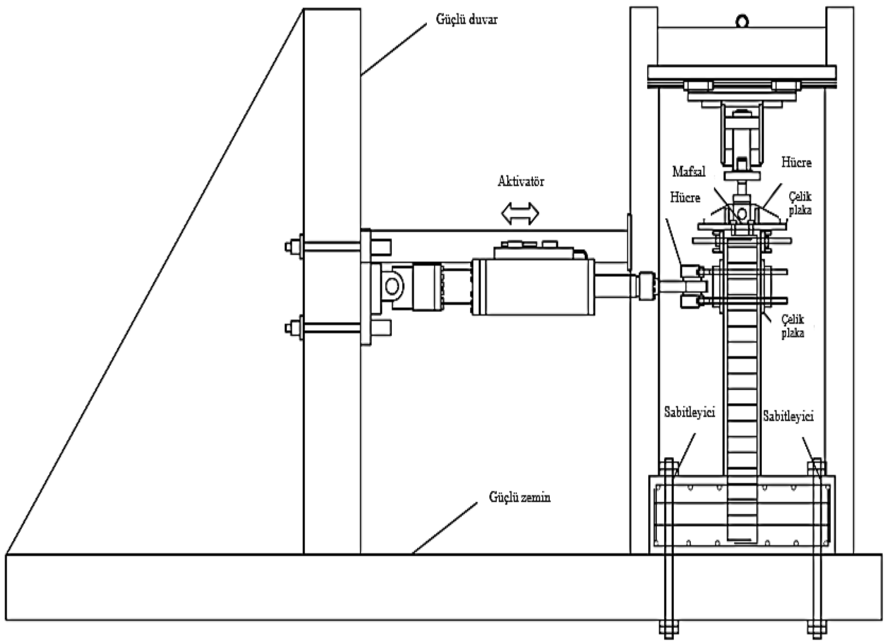

Figure 3.2: Test layout

Figure 3.1: General properties of the test sample

b/h (cm/cm)	*30/30*
a/d	*4.5*
f_{ck} (MPa)	*32.5*
$f_{yk}/f_{su}/f_{ywk}$ (MPa)	*480/640/690*
Longitudinal reinforcement (ratio)	*6ϕ14 (0.01)*
Transverse reinforcement (ratio)	*ϕ8/10 (0.008)*
Axial load, N (kN)	*292.5*
Axial load without dimension	*0.10*

Changes in the displacement, axial load and torque applied to the test sample according to the cycle number are shown in Figure 3.3 (a~c). Fixed axial load and variable moment effects applied to the sample can be seen on the analytic M-N interaction diagrams (interaction diagrams obtained with the help of moment curvature analysis and nominal capacity) given in the Figure 3.3(d).

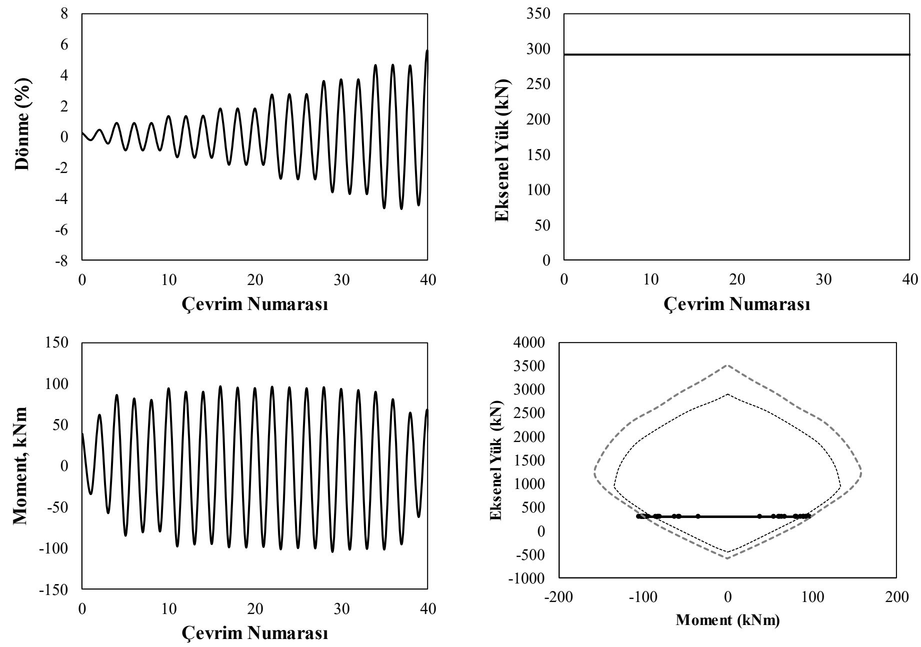

Figure 3.3: (a) the demand for rotation in the displacement controlled cyclical loading, (b) the axial loading, (c) the bending moment demand in the cyclic load, (d) the representation of the experimental results on the analytical N-M interaction diagram, on the test sample.

The test sample collapse is shown by the photographs in Figure 2.7.

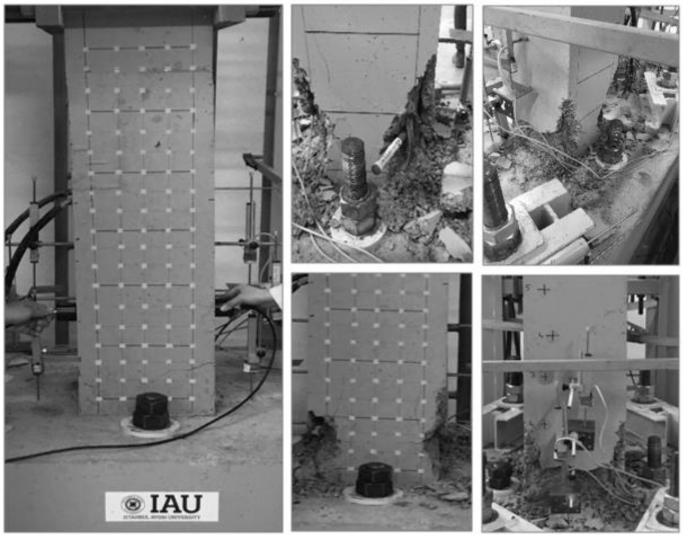

Figure 3.4: Photographs of the collapsed test sample during and at the end of the loading

In the cyclical loading steps applied to the test sample, the average pressure reduction of the experimental horizontal load, determined by the displacement gauges placed in the vertical position in the support region, is given in Figure 3.5.

As can be seen in the figure, the increasing pressure reinforcement unit shortening due to the increased displacement amplitude demand causes buckling of the reinforcement and a significant decrease in the load bearing power. In the case of longitudinal reinforcements of the column sample in the pressure zone, the buckling is markedly visible on the figure, where the buckling occurs visibly and the load-bearing capacity is reduced by about 20%. The analytical buckling unit deformation limit, which is also calculated by the relation of (1), is also shown in the dashed line on the diagram. As can be seen from the figure, the analytical buckling limit of pressure reinforcement (0.0243) results close to the experimental buckling unit shortening (0.0268).

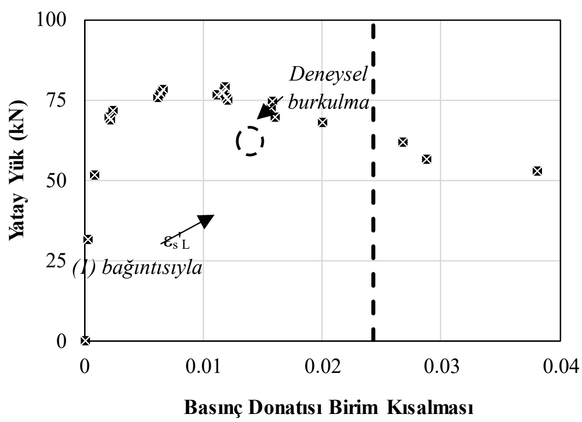

Figure 3.5: Comparison of experimental load-pressure reinforcement unit deformation request and analytical buckling deformation limit with experimental results

5. Other Experiments

In the comparison of the analytical buckling limit with experimental results, experimental results of 40 column samples tested by various researchers were used. The general characteristics and experimental results of the column samples taken from the experimental database were taken from the reinforced concrete column database study prepared by the University of Washington.**[12]** The analysis intervals of the basic design variables of the reinforced concrete columns in the experimental database are summarized in Figure 3.2.

Figure 3.2: Basic design variables and observation intervals of column samples in experimental database

Parameter	Minimum	Maksimum
Concrete compressive strength, f_{ck} (MPa)	23.1	102.2
Longitudinal reinforcing steel yield strength, f_{yk} (MPa)	308	896
Transversal reinforcing steel yield strength, f_{ywk} (MPa)	255	890
Slenderness ratio, L/h	1.5	10
Longitudinal reinforcement ratio, $\square_t$	0.0046	0.0362
Volumetric ratio of transverse reinforcement, $\square_h$	0.0034	0.0153
Axial load level, $N/(Af_{ck})$	0.1	0.7

A comparison of the analytical and experimental results of the column samples taken into account in the experimental database will be done on load displacement relations. In the study, SeismoStruct [13] software was used to determine the analytical load displacement relationships of the test samples. The modeling details applied in determining the analytical load displacement relationships can be seen in [14]. Figure 3.6 shows the analytical and experimental load displacement relationships for a column sample based on the experimental database.

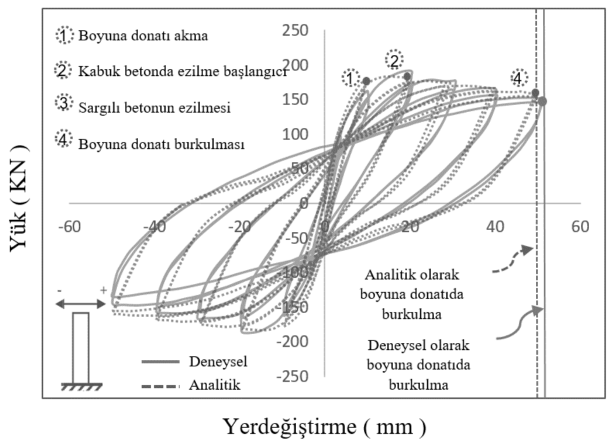

Figure 3.6: Experimental and analytical load displacement relationships (Ang vd., 1981.No.3) for a column sample in the experimental database

In the comparison of Figure 3.6, the analytical load displacement relationship (1) is limited by the analytical buckling damage limit determined by the correlation. The experimental displacement where the buckling of the compression reinforcement observed is 50mm and the analytical displacement obtained by the analytical buckling damage limit approach is 48.8 mm. Analytical and experimental buckling displacements are calculated for all columns in the experimental database and the results are summarized in Figure 3.3.

Figure 3.3: Comparison of analytical and experimental buckling displacements of column samples in experimental database

Column name/Reference	Experimental displacement corresponding to buckling damage limit (mm)	Analytical displacement corresponding to the buckling damage limit determined by (1) (mm)
No.1/ Ang vd. ***[15]***	*60*	*59*
No.2/ Ang vd.	*52*	*60*
No.3/Ang vd.	*50*	*49*
No.4/Ang vd.	*58*	*66*
*No.3/ Soesianawati vd.****[16]***	*45*	*45*
No.4/ Soesianawati vd.	*41*	*40*
No.1/Tanaka ve Park ***[17]***	*120*	*128*
No.2/Tanaka ve Park	*87*	*83*
No.3/Tanaka ve Park	*59*	*59*
No.4/Tanaka ve Park	*80*	*78*
No.5/Tanaka ve Park	*74*	*67*
No.6/Tanaka ve Park	*67*	*66*
No.7/Tanaka ve Park	*82*	*74*
No.8/Tanaka ve Park	*78*	*77*
No.9/Park ve Paulay ***[18]***	*84*	*94*
No.A1/Wehbe vd. ***[19]***	*122*	*131*
No.A2/Wehbe vd.	*102*	*93*
*No.1/Nosho vd.****[20]***	*37*	*34*
BG-2/Saatcioglu ve Grira	*82*	*84*
BG-9/ Saatcioglu ve Grira	*66*	*64*
No.11/ Watson ve Park	*36*	*35*
NIST ,Model N3 ***[23]***	*102*	*102*
No.A2/ Kunnath vd, ***[24]***	*68*	*66*
No.A4/ Kunnath vd.	*57*	*55*
No.A5/ Kunnath vd.	*75*	*64*
No.A9/ Kunnath vd.	*63*	*65*
No.SRPH1/ Kunnath vd.	*320*	*274*
*FL1 / Kowalsky vd.****[25]***	*332*	*309*
FL2 / Kowalsky vd.	*210*	*202*

Figure 3.3: Comparison of analytical and experimental buckling displacements of column samples in experimental database (Continued)

Column name/Reference	Experimental displacement corresponding to buckling damage limit (mm)	Analytical displacement corresponding to the buckling damage limit determined by (1) (mm)
FL3 / Kowalsky vd.	*340*	*340*
No415/ Lehman ve Moehle ***[26]***	*127*	*109*
No815/ Lehman ve Moehle	*445*	*416*
No1015/ Lehman ve Moehle	*635*	*607*
No407/ Lehman ve Moehle	*127*	*131*
No430/ Lehman ve Moehle	*178*	*147*
No.328/Calderone vd. ***[27]***	*125*	*125*
No.828/Calderone vd.	*600*	*585*
No .Col1/Nelson ***[28]***	*48*	*42*
No .Col2/Nelson	*57*	*50*
No .Col3/Nelson	*48*	*55*
No .Col4/Nelson	*45*	*45*

The comparison of analytical and experimental results can be seen in Figure 3.7. As can be seen from the figure, the displacements obtained by the deformation of the buckling damage limit pressure reinforcement obtained by the relation of (1) are very close to the experimental results.

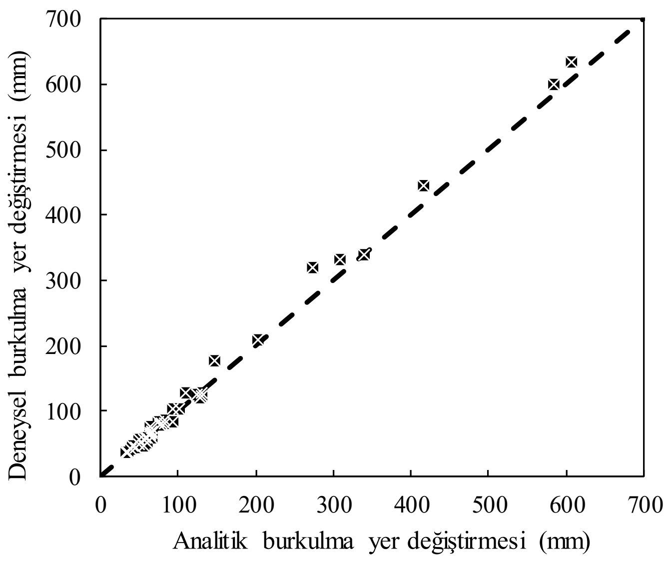

Figure 3.7: Comparison of analytical and experimental buckling displacements of column samples in experimental database

6. Conclusion

In this study, the comparison of the upper limit of analytical unit shortening with the results of the relation of (1) for the buckling damage limit in reinforced concrete structural elements was compared with the experimental results. In the comparisons, the comparative analysis of the (1) relationship of the single reinforcing bar specimens forced under axial pressure with the help of the experimental results was compared to the axial load and the realism of the reinforced concrete column samples that were forced to simulate the earthquake loading under cyclical horizontal load. The basic results obtained from comparisons based on a limited number of test samples are summarized briefly below.

In the laboratory of İstanbul Aydın University Department of Civil Engineering, the analytical buckling stresses determined by the experimental and (1) relation for the sample tested with constant axial load and reversible-cyclical loading are very close to each other (See Figure 3.5). The relative error rate between experimental and analytical unit shortages is 9%.

The experimental results of a total of 40 column samples tested by fixed investigators with fixed axial load and reversible-cyclic displacement loading are closely related to the analytical buckling damage displacement capacities determined by the relation of the experimental results with (1) (Figures 3.2 and 3.7). The relative error rate between experimental and analytical buckling damage limit displacement capacities for columns in the experimental database is maximum 17%, minimum -16% and average 2.5%.

Depending on the comparison results of the study, it can be said that the analytical buckling unit deformation limit, which can be determined by the relation of (1), is generally close to the experimental results for the fixed-axial load and the reversible-cyclic displacement loading situation with increasing amplitude. It is also recommended to compare the analytical buckling unit-deforming limit for samples with different loading history.

References

[1] Mau, S.T. and El-Mabsout, M., Inelastic Buckling of Reinforcing Bars, 1989, ASCE, J. Eng. Mech., 115(1): 1-17.
[2] Monti, G., and Nuti, C. Nonlinear cyclic behavior of reinforcing bars including buckling. J. Struct. Eng.,1992 118(12), 3268–3284.
[3] Gomes, A., and Appleton, J. Nonlinear cyclic stress-strain relationship of reinforcing bars including buckling, 1997, Eng. Struct., 19(10), 822–826.
[4] Rodriguez, M., Botero, J., and Villa, J. Cyclic stress-strain behavior of reinforcing steel including effect of buckling, 1999, J. Struct. Eng., 125(6), 605–612.
[5] Yalçın, C., and Saatçioğlu, M., Inelastic Analysis of Reinforced Concrete Columns,Computers and Structures, 2000, No. 8, 539-555.
[6] Moyer, M., and Kowalsky, M., Influence of tension strain on buckling of reinforcement in RC bridge columns, 2001, Dept. of Civil Engineering, North Carolina State Univ. , Raleigh, N.C.
[7] Hose, Y. D. Seismic performance and failure behavior of plastic hinge regions in flexural bridge columns, 2001, PhD dissertation, Dept. Of Structural Engineering, Univ. of California, San Diego.

[8] Bae, S., Seismic Performance of Full-Scale Reinforced Concrete Columns, 2005, Ph.D. thesis, The University of Texas at Austin.

[9] Mieses, A.M., Inelastic Buckling Behavior of Concrete Reinforcing Bars under Monotonic Uniaxial Compressive Loading, 2002, M.S. thesis, The University of Texas at Austin.

[10] Aydemir, C , Eser Aydemir, M., Betonarme Kirişlerin Hasar Sınırlarının Deneysel Gözlemlerle İrdelenmesi, 2017, Teknik Dergi, 28 (4), 8023-8049.

[11] Dhakal, R.P. and Maekawa, K., Reinforcement Stability and Fracture of Cover Concrete in Reinforced Concrete Members, 2002, Journal of Structural Engineering, ASCE, 128(10):1253-1262.

[12] Berry, M.P. and Eberhard, M.O., A Practical Performance Model for Bar Buckling, 2005, Journal of Structural Engineering, ASCE, 131(7):1060-1270.

[13] Seismosoft, SeismoStruct v7.0 – A computer program for static and dynamic nonlinear analysis of framed structures, 2014, available from http://www.seismosoft.com.

[14] Ghulam Mostafa WAZIRY, Betonarme Kolonlarda Burkulma Hasar Limiti, 2018, Yüksek lisans tezi, Istanbul Aydın Üniversitesi, Fen Bilimleri Enstitüsü.

[15] Ang Beng G., Priestley, M.J.N., and Park, R., Ductility of Reinforced Bridge Piers Under Seismic Loading, Report 81-3, Department of Civil Engineering, University of Canterbury, Christchurch, New Zealand, February 1981.

[16] Soesianawati, M.T., Park, R., and Priestley, M.J.N., Limited Ductility Design of Reinforced Concrete Columns, Report 86-10, Department of Civil Engineering, University of Canterbury, Christchurch, New Zealand, March 1986.

[17] Tanaka H., and Park R., Effect of lateral confining reinforcement on the ductile behavior of reinforced concrete columns. Report 90-2, Department of Civil Engineering, University of Canterbury, June 1990, 458 pages.

[18] Park, R., and Paulay, T., Use of Interlocking Spirals for Transverse Reinforcement in Bridge Columns. Strength and Ductility of Concrete Substructures of Bridges, RRU (Road Research Unit) Bulletin 84, Vol. 1, 1990, pp. 77-92.

[19] Wehbe, N., and Saiidi, M.S., and Sanders, D., Confinement of Rectangular Bridge Columns for Modrate Seismic Areas, 1998, National Center for Earthquake Engineering Research (NCEER) Bulletin, 12(1).

[20] Nosho, K., Stanton, J., and MacRae, G., Retrofit of Rectangular Reinforced Concrete Columns using Tonen Forca Tow Sheet Carbon Fiber Wrapping, 1996, Report No. SGEM 96-2, Department of Civil Engineering, University of Washington, Seattle.

[21] Saatcioglu, M., and Grira, M., Confinement of Reinforced Concrete Columns with Welded Reinforcement Grids, 1999, ACI Struct. J., 96(1), 29-39.

[22] Watson, S., and Park, R., Design of Reinforced Concrete Frames of Limited Ductility, 1989, Report 89-4, Department of Civil Engineering, University of Canterbury, Christchurch, New Zealand.

[23] Cheok, G.S., and Stone, W.C., Behavior of 1/6-Scale Model Bridge Columns Subjected to Cycle Inelastic Loading, 1986, NBSIR 86-3494, U.S. National Institute of Standards and Technology, Gaithersburg, Maryland.

[24] Kunnath, S., El-Bahy, A., Taylor, A., and Stone, W., Cumulative Seismic Damage of Reinforced Concrete Bridge Piers, 1997, Technical Report NCEER-97-0006, National Center for Earthquake Engineering Research, Buffalo, New York.

[25] Kowalsky, M.J., Priestley, M.J.N., and Seible, F., Shear and Flexural Behavior of Lightweight Concrete Bridge Columns in Seismic Regions, 1999, ACI Struct. J., 96(1),136-148.
[26] Lehman, D.E., and Moehle, J.P., Seismic Performance of Well-Confined Concrete Bridge Columns, 2000, Pacific Earthquake Engineering Research Center Report 1998/01, University of California, Berkeley, California.
[27] Calderone, A.J., Lehman, D.E., and Moehle, J.P., Behavior of Reinforced Concrete Bridge Columns Having Varying Aspect Ratios and Varying Lengths of Confinement, 2000, Pacific Earthquake Engineering Research Center Report 2000/08, University of California, Berkeley, California.
[28] Nelson, Jared M., Damage Model Calibration for Reinforced Concrete Columns, 2000, Master's Thesis, Department of Civil and Environmental Engineering, University of Washington, Seattle.

INTERNATIONAL JOURNAL OF ELECTRONICS, MECHANICAL AND MECHATRONICS ENGINEERING
Vol.9 Num.1 - 2019 (1637-1645)

Risk Analysis of Slaving Floor in Construction Sites

Sepanta NAİMİ[1], Houda HRİZİ[2]

Abstract: This study allows the application of tools for the analysis and prevention of natural risks of a real project. The importance of introducing the actors and the main stages of risk management and the difference between risk and uncertainty are emphasized. The aim of the study is to detect the risk and its location diligently, and determine if there is a risk of slippery ground on the site. In this study, Ghandouri project is described around a geotechnical analysis that confirms the existence of different stages and the risk of slippage in a practical situation. Current paper attempts to eliminate the risk by analyzing the soil and using Talren and Slop programs and offers a solution to ensure the stabilization of the site found.

Keywords: *Risk analysis, construction site, geotechnical analysis, slippery ground.*

İnşaat Şantiyelerde Kaygan Zeminin Risk Analizi

Öz: Bu araştırmada, hakiki bir projenin doğal risklerinin analizi ve önlenmesi için araçların uygulanmasına izin verildi. Aktörlerin ve risk yönetiminin ana aşamalarının tanıtılması ve risk ile belirsizlik arasındaki farkın önemi vurgulandı. Çalışmanın amacı, riski ve yerini netleştirerek dikkatle hazırlanması ve inşaat şantiyede kaygan zemin riski bulunduğunun keşfedilmesidir. Bu araştırmada, Ghandouri projesi pratik bir durumda farklı aşamaların varlığını ve kayma riskini doğrulayan bir jeoteknik analiz etrafında tanımlanmaktadır. Daha sonra, toprağı analiz ederek ve Talren ve Slop programlarını kullanarak, risk atlatılmaya çalışıldı ve sitenin dengelenmesini sağlamak için bir çözüm bulundu.

Anahtar Kelimeler: *Risk analizi, inşaat şantiyesi, jeoteknik analizi, kaygan zemin.*

[1] Corresponding author: sepanta.naimi@gmail.com, Civil engineering dept., Istanbul Aydin University, Istanbul, Turkey, https://orcid.org/0000-0001-8641-7090
[2] Civil engineering dept., Istanbul Aydin University, Istanbul, Turkey, https://orcid.org/0000-0003-0575-0786

1. Introduction

The construction projects in Morocco often suffer from delays or over budgeting due to costs and deadlines not being properly implemented, mismanagement and disregard of risks in the project.

Corrective and preventive measures should be taken against certain risks in the workplace. Taking correct measures can only be possible with accurate and complete identification of hazards and the risks that may arise as a result. Risk assessment should not be expected to destroy the hazards in a workplace in a short time. Risk is a concept that eastern culture is not familiar with; to the point that there is no equivalent word in related languages. It is often confused with the concept of uncertainty. Corporate risk management is a set of activities that can be summarized as the recognition of existing risks of institutions, measuring their risks, prioritizing them, deciding the methods of responding to risks, reporting their activities related to risks and taking measures for continuous review.

The gravity, slope, water and similar value of a slope of ground cause serious damage to the structures due to the forces and outward movements. In addition, these factors have effects in terms of economy, all of which lead to loss of money and even lives. The movements affecting the slopes are extremely diverse in terms of their size, morphology and kinematic yield, they cause not only the superficial movements on the road, but also in part or in total destruction.

2. Risk analysis safety coefficient and balance calculation

The present analysis of the stable condition of the soil is regulated by looking at the two dimensions of the slope to examine the equilibrium conditions of the monolithic soil mass confined to the surface of a soil gap and the slits formed due to interstitial pressures and possible external loads along the tearing surface formed by the mass of the massive mass.

Table 1: Values related to safety coefficient:

Method	Hypotheses	Balancing Calculations	Unknown Calculations
Unending slit	• Infinite extent; • The fracture surface is parallel to the surface of the base of the slope	∑ Forces perpendicular to the slope. ∑ forces parallel to the slope.	• Coefficient of safety • The normal force at the base
Fellenius Method	-The breaking surface is circular. -The forces on the side of the slices are neglected.	∑ Central moment force of slipping.	• Factor of safety
Bishop simplified	• The power of soil collapse • The strength of the side sections is horizontal. (There is no break between the sections).	∑ moments from the center of the slip circle. ∑ Horizontal power	• Factor of safety • The normal force (N) at the base of the fracture surface.

Fellinus Method: This method is the first advanced soil partitioning calculation method. The simplicity of this method is that the safety coefficients can be calculated by the hand measure (Meter Accounting).

Bishop Method (1955): A method of calculating the type of landslide on a given line.
Unending slit: The area of the slit is parallel to the collapse area. The safety coefficient is normal power.

3. Implementation example

This problem is located in the north-west of Tangier in Morocco, spread over 60 hectares of land, this is a coastal strip in an unstable sea. This area is located 3 km from the city center and 15 km from TANGIER Airport. Based on the geological maps in the TANGIER region, we can see the predominant facies are clays and gray schistose marls, yellow in weathering, dated Senonian, but we also find Paleocene in comparable facies, white marl Eocene, and Oligo-Miocene marly facies and horizons of sandstone.

In order to determine the soil type of the study area, we carry out the tests with the presyo metric tests in place. Tangier has a semi-humid climate, with a rainfall of 800 mm and an approximate temperature of about 17.5 ° C. Rainfall varies over time from 500 to 1200 mm, and in the space from 750 to 1000 mm. Winter months (rainfall over 100mm) continue from November to March. Average number of rainy days per year is 90, equivalent to 3 months. Prolonged precipitations (24-hour sequence) are exceptional, often lasting only a few hours, and short showers may be relatively severe (more than 100mm / s for 15-minute showers).

- These conditions can cause significant leakage which may impair the stability of the land.
- The concise tests indicate the presence of water in the finished boreholes from the surface circulation of the source rain water.

4. The Encountered Risks in the Project

There were landslides during the site investigation, and the effect of this phenomenon can be observed on the land in the field of study. The first constraint encountered in the investigated land is that it consists of two slopes that are connected to each other by a small platform.

As can be seen, various risks were encountered and prioritized at this construction site and the region was geo-technically studied in order to identify and prevent these risks. In addition, the geological and hydrogeological studies of the site are known; comfort modalities that are most suitable for the site to stabilize the existing structures are required to be proposed and also an investigation of the slope is needed.

5. Laboratory Tests

Identification tests were performed on the ground in a private construction laboratory.

The results of the tests are given in the tables below:

Table 2: Determination of the water content and density of soils

Reference Sample	Sampling Method	Preservation Condition	Steaming Temperature	Water Content	Density ρ (kg /m^3)
SP01 (1,50 to 2,00) m	Intact	box	105°C	21	
SP01 (5,00 to 5,20) m	Intact	box	105°C	16	
SP01 (9,5 to 10,0) m	Intact	box	105°C	15	
SP01 (11,0 to 11,50) m	Intact	box	105°C	11	2201

Table 3: Cone Liquidity Limit, Roll Plasticity

Reference Sample	Sampling Method	Preservation Condition	Limit of Liquidity WL(%)	Limit of Plasticity WP(%)	Index of Plasticity IP(%)
SP01 (1,50 to 2,00) m	redesigned	box	47	26	21
SP01 (5,00 to 5,20) m	redesigned	box	46	24	22
SP01 (9,5 to 10,0) m	redesigned	box	41	21	20
SP01 (11,0 to 11,50) m	redesigned	box	42	21	21

Table 4: Particle size analysis by dry sieving after washing

Reference Sample	D max (mm)	>50 mm	>2mm	2mm to 80 µm	<80µm
SP01 (1,50 to 2,00) m	63,0	0	2	2	96
SP01 (5,00 to 5,20) m	31,50	0	8	3	89
SP01 (9,5 to 10,0) m	40,00	0	13	5	82
SP01 (11,00 to 11,50) m	12,50	0	1	3	96

Table 5: Determination of soil moisture content and density

Reference Sample	Sampling Method	Preservation Condition	Steaming Temperature	Water Content	Density ρ (kg /m^3)
SP3 (3,50 to 4,00) m	Intact	box	105°C	19	2140
SP3 (8,00 to 8,50) m	Intact	box	105°C	22	2048

Table 6: Cone Liquidity Limit, Roll Plasticity

Reference Sample	Sampling Method	Preservation Condition	Limit of Liquidity WL(%)	Limit of Plasticity WP(%)	Index of Plasticity IP(%)
SP3 (2,00 to 2,50) m	redesigned	box	41	23	18
SP3 (3 ,50 to 4,00) m	redesigned	box	47	25	22
SP3 (8 ,0 to 8,5) m	redesigned	box	41	23	18

Table 7: Particle size analysis by dry sieving after washing

Reference Sample	D max (mm)	>50 mm	>2mm	2mm to 80 µm	<80µm
SP3 (2,00 to 2,50) m	6,30	0	0	2	98
SP3 (3,50 to 4,00) m	6,30	0	0	1	99
SP3 (8,0 to 8,5) m	14,00	0	2	0	98

Table 8: CD Shear Test

Reference Sample	C'	φ'	Cr'	φr'
SP01 (5,00 to 5,20) m	20	24	20	24
SP01 (8,00 to 8,50) m	23	26	23	26

Table 9: CD Shear Test

Reference Sample	C'	φ'	Cr'	φr'
SP3 (3,50 to 4,00) m	22	24	22	24

Table 10: Odometric Test

Reference Sample	Internal	Pc(Kpa)	Ig	Pg(Kpa)
SP3 (3,50 to 4,00) m	0,096	45	0,042	20
SP3 (8,0 to 8,5O) m	0,142	220	0,06	28,33

6. Definition of Talren Logistics with Soil Gravity Balance Calculation

The analysis of the equilibrium calculation of the soil gravity processes was conducted to determine the centralized soil displacement. The analysis of the irregularly three-zone landslide analysis is very important. Talren geo is a balance control logistics operation used in technical studies. This arrangement is defined as strengthening or non-reinforcement [11]; Talren interface; the Talren 4 method has two important organizational distinctions: Data type: All elements used in describing our project should be: Geometric data, ground data, soil loading data and soil strengthening. Phase calculation method: All phases and calculations to be used in construction and account arrangement results should be seen.

7. Account and control

Three calculations are divided into three parts on the construction site by using three separate calculations in each section of the earthquake effect and whether the security coefficient is calculated and the safety coefficient in three parts is lower than 1.5.

The following table shows the properties of the modeling:

Table 11: properties of the modeling

References	Top side	Definition
1 – FILLING	0.00 m	Volumetric weight: 18.0 kN / m³ Non-measurable volumetric weight: 10.0 kN / m³ Internal friction angle: 20 degrees Combination: 0.00 kN / m²
2 – CUTTING FROM THE TOP SOIL	-3.49 m	Volumetric weight: 18.0 kN / m³ Non-measurable volumetric weight: 10.0 kN / m³ Internal friction angle: 16 degrees Combination: 4.00 kN / m²
3– Stone sedimentation content	-11.10 m	Volumetric weight: 18.9 kN / m³ Non-measurable volumetric weight: 10.0 kN / m³ Internal friction angle: 27 degrees Joint angle: 15.00kN / m²

8. Regulation Methods Application

Retaining wall pre-measurement methods

After the risk analysis and calculation of our site, the risk ratio of slippery ground seems high and we suggested a solution and we could reduce the risk by holding the retaining wall. The retaining wall should be constructed to carry out three-zone research at a height of approximately 11.1 m to prevent water leaking from the soil. This level should be constructed by taking the necessary precautions for the landslides and sewing the concrete piles. The length of the concrete pile to be drilled into the soil should be 11,5 m. The retaining wall cannot be used if it does not exceed 7 m. Following are the measurements of the Retaining Wall: B = 5,12 m, b = 0,15 m, e = 0,92 m, a = 0,64 m, h = 0,925 m, L = 7 m, H = 11,5 m

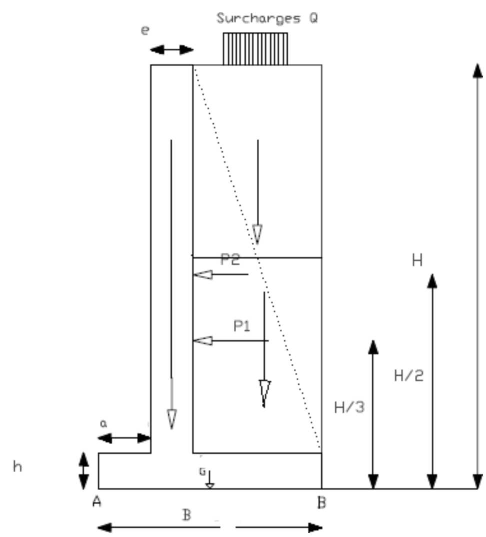

Figure 1: Retaining wall pre-measurement

As a result of this study, a long height should be given for vertical measurement of the retaining wall constructed, a very wide threshold and water pressure and terracing in the soil should be made. This can happen because the soil structure has deteriorated since the soil is already in the flood layer. Large risks can be avoided by using other methods.

In this case, only two solutions should be considered:
Solution: It is necessary to measure the terracing of the ground hole, the perforated wall side section and the soil gold. All hitting soils must be fixed with iron poles.

Note: A drainage system should be established when there is soil movement. In this case, the hole must be drilled in the soil. Protective measures should be taken when necessary.

9. Concrete pile

In this case, after making the risk analysis and calculation of our site, which should be (25 m in depth) and (150 cm in diameter) and should have a load capacity of 15 tons and 1000 tons, it is necessary to excavate and lay out the deep foundation necessary for the iron pile driving to a field.

In this project, we proposed a solution to the concrete pile and the analysis, control, and stakes were performed on the ground using the SLOP program to implement it.

10. SLOPE / W Computer program presentation:

SLOPE / W is a computer program that is performed by GEO-SLOPE International Canada for the analysis of the land grab calculation. This computer program is a method of measuring the controversial final balance limits mentioned in the previous sections. In this program, you can use the arrangements of the finished works but the modeling can be done with the help of SIGMA W. This computer program also calculates the safety coefficients of, for example, planar or non-planar samples of terracing methods. In contrast, planar terracing methods are automatically investigated in the mentioned program.

SLOPE / W computer calculation has many methods of calculation, Normal, Bishop, Janbu general, Spencer, Morgenstern, Price, Winding, and Lowe Karafiath which are used in the calculation methods of security coefficient. SLOPE / W Geostudio 2002 program is integrated with various other programs. The final equilibrium theory of the slope safety coefficient is calculated here. With the use of this program simple and complex slope security coefficient problem resolution methods and Microsoft Windows XP program graphics and calculation programs can be discussed.

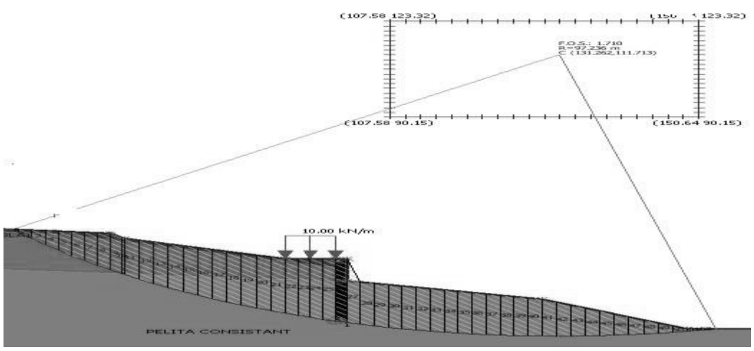

Figure 2: SLOPE model in

11. Comparison of risk rates before and after implementation of the solution:

Table 11: Risk rates before applying the solution in three areas

	Constant Coefficient	Ground cover when there is no earthquake effect		Ground cover when there is earthquake effect	
		Coefficient	Risk ratio %	Coefficient	Risk ratio %
Area 1	1,5	0,878	42%	0,592	60%
Area 2	1,5	0,84	44%	0,56	62%
Area 3	1,5	1,25	16,66%	0,73	42%

In the above table, we have found the coefficient and the rate of risk in the construction site. The table shows the risk of high landslide in all regions. A test which was conducted with sloppy program was applied to reduce the rate of concrete piles, after the application the risk has fallen as follows:

Table 12: Risk rates after the implementation of the solution

	Constant Coefficient	Safety coefficient	Risk ratio%
Region 1	1,5	1.710	0%
Region 2	1,5	1.822	0%
Region 3	1,5	1.541	0%

According to the results, the safety coefficient is higher than the constant coefficient, reducing the risk, and in this case, the risk is reset. To this date, concrete pile continues to be the best solution to reduce landslide despite its expensive cost, and it is recommended to be used as a solution for large projects located in slippery areas (coastal or mountainous areas etc.).

12. Conclusion

In order to overcome the risk of soil slippage, two solutions are suggested, retaining wall and bored pile application, but in this project concrete pile is preferred because after the analysis it was determined that the retaining wall is reversed.

After making two different designs, the financial cost difference between the retaining wall and the concrete pile is compared. In order to do this, all measurements of the retaining wall and the concrete pile were taken and the costs of both concrete and steel was calculated for each cubic meter. The results showed that the total cost of retaining wall was € 123.347, and the total cost of concrete pile was 188.559 €.

The cost of concrete pile is higher compared to that of the retaining pile, however in order to ensure the safety of the tourism project as well as the lives of the tenants and protect them from any future danger, the owner deemed it necessary to apply the concrete pile technique.

References

[1] Beer M, Zhang Yi, Tong Quek S, Phoon KK. Reliability analysis with scarce information: Comparing alternative approaches in a geotechnical engineering context. Struct Saf 2013;41:1–10.

[2] Ching Jianye, Phoon Kok-Kwang. Correlations among some clay parameters — the multivariate distribution. Rev Can Geotech J 2014;51(6):686–704. https://doi.org/ 10.1139/cgj-2013-0353.

[3] Hutchinson TPTP, Lai CD. Continuous bivariate distributions emphasising applications (No. 04; QA278, H8.). 1990.

[4] Ang, A.H.S., Tang, W.H., 2007. Probability Concepts in Engineering: Emphasis on. Applications to Civil and Environmental Engineering, Seconded. John Wiley & Sons.

[5] Xu, L., Coop, M.C., Zhang, M.S., Wang, G.L., 2018. The mechanics of a saturated silty loess and implications for landslides. Eng. Geol. 236, 29–42.

[6] Zhang, W.G., Goh, A.T.C., Xuan, F., 2015. A simple prediction model for wall deflection caused by braced excavation in clays. Comput. Geotech. 63, 67–72.

[7] Zhang, J., Wang, H., Huang, H.W., Chen, L.H., 2017. System reliability analysis of soil slopes stabilized with piles. Eng. Geol. 229 (7), 45–52.

[8] Wang, Y., Cao, Z.J., Au, S.K., 2010. Efficient Monte Carlo simulation of parameter sensitivity in probabilistic slope stability analysis. Comput. Geotech. 37 (7–8),
1015–1022.

[9] Kaya Özlem, Türk İnşaat Sektöründe Risk Analizi ve Yönetiminin Araştırılması,yüksek lisans tezi,2010,Yıldız teknik üniversitesi.

[10] Latif Onur UĞUR, İnşaat sektöründe riskler ve risk yönetimi, Yük. İnş. Müh.tezi,2006,İstanbul üniveritersi.

[11] Doç.Dr.Selim Altun, zemin iyileştirme yöntemleri derin temeller ve uygulama örnekleri,inş.Müh.geoteknik ana bilim dalı.2010.

[12] Office of Project Management Process Improvement, Project Risk Management Handbook, First Edition, June 26, 2003, Sacramento.

INTERNATIONAL JOURNAL OF ELECTRONICS, MECHANICAL AND MECHATRONICS ENGINEERING
Vol.9 Num.1 - 2019 (1647-1656)

A Review of Shear Resistance of Rockfill Using Large Scale Shear Tests

Kaveh Dehghanian[1], Sayed Mansoor ZAFAR[2], Emrah ÇALTILI[3]
Beste KOÇAK DİNÇ[4], Hakan Murat SOYSAL[5]

Abstract: Earth and rockfill dams, because of their special characteristics compared to concrete dams, are widely used in construction throughout the world. Rockfill dams are more flexible, have capacity to absorb large seismic energy, and adaptability to various foundation conditions. The use of modern earth and rock equipment and locally available materials make such dams economical as well. Therefore, improving the knowledge of experts about the design and maintenance of these dams are vital. Different reports of settlement and deformation of operating rockfill dams depict the importance of technique improvements and designing new test apparatus to monitor them.

The behavior of these materials, specifically their shear strength are not fully understood. Several types of laboratory devices have been developed to estimate the strength of these materials. Among these devices, direct shear test has been employed most commonly owing to its simplicity and low-cost compared to triaxial and other methods. Traditional laboratory direct shear tests are not appropriate for investigation of rockfill materials which have large-sized particles. In this case, laboratory large scale direct shear tests are required to be performed on these materials. In this paper, a brief review of parameters affecting shear resistance of these particles and a history of large scale tests are presented.

Keywords: *Shear strength, direct shear test, rockfill material, shear resistance*

[1]Assistant Professor, Civil Engineering department, Istanbul Aydın University, Turkey
Corresponding author: kavehdehghanian@aydin.edu.tr
[2]Msc Student, Civil Eng. Department, Istanbul Aydin University, Istanbul, Turkey
[3]Professional Engineer, Civil Engineering department, Istanbul Aydın University, Turkey
[4]Professional Engineer, Civil Engineering department, Istanbul Aydın University, Turkey
[5]Geological Engineer, Civil Engineering department, Istanbul Aydın University, Turkey

1.Introduction

Testing large granular particles require a large test apparatus to avoid scale effects related to the size of particles compared to the dimension of test apparatus. In practice, performing such tests with controlled loading simulating the site condition is difficult so most of the tests have been performed in small scales which does not reflect the factual situation. Empirical models have been developed to predict the strength of rockfill utilizing available parameters but the reliability of them are not clear. These parameters influence the shear strength, and thus the friction angle (Ø). The shear strength of rockfill may vary directly with normal effective stress, dry density, particle roughness, particle crushing strength and inversely with grain size, uniformity of grading, and particle shape (Marsal, 1973). In a laboratory specimen, the maximum particle size (d) is determined according to the minimum dimension of the specimen (D). There are four different methods for preparing laboratory specimens; namely, parallel gradation technique, scalping method, quadratic gradation curve method and replacement technique (Varadarajan, 2003). The first two methods, commonly used by engineers, were adopted to investigate the effect of particle size on direct shear test. In the parallel gradation technique, the reduced particle-size laboratory specimens were formed with size distributions parallel to that of the original sampled material as it can be seen in Figure 1. In the scalping method, all particles considered oversize were removed (scalped) from the original material. Indeed, scalped gradation is considered for testing as equivalent grading instead of the original one. These techniques were used to determine the gradation of specimens in the tests and the numerical simulations related to the scale of shear boxes (Bagherzadeh, 2009). In both methods, a fraction of the representative gradation will be ignored which influences the shear strength characteristics of the base soil (Hamidi, 2012).

The maximum particle sizes of samples are being selected based on the dimension of the boxes according to ASTM-D3080. According to ASTM, the minimum specimen diameter for circular specimens, or width for square specimens, shall be 2.0 in. [50 mm], or not less than ten times the maximum particle size diameter, whichever is larger. The minimum initial specimen thickness shall be 0.5 in. [13 mm], but not less than six times the maximum particle diameter. The minimum specimen diameter to thickness or width to thickness ratio shall be 2:1. Jewell and Wroth (1987) suggested a ratio of shear box length to average particle size in the range of 50 to 300. According to Japanese standards, there are three approaches to determine the maximum allowable particle size for a large shear box test: a) 1/10–1/5 of the box length, (b) 1/7–1/5 of the box height, and (c) 1/9–1/5 of the smaller of the box length or height, among which the appropriate size is selected (Lee et al, 2009).

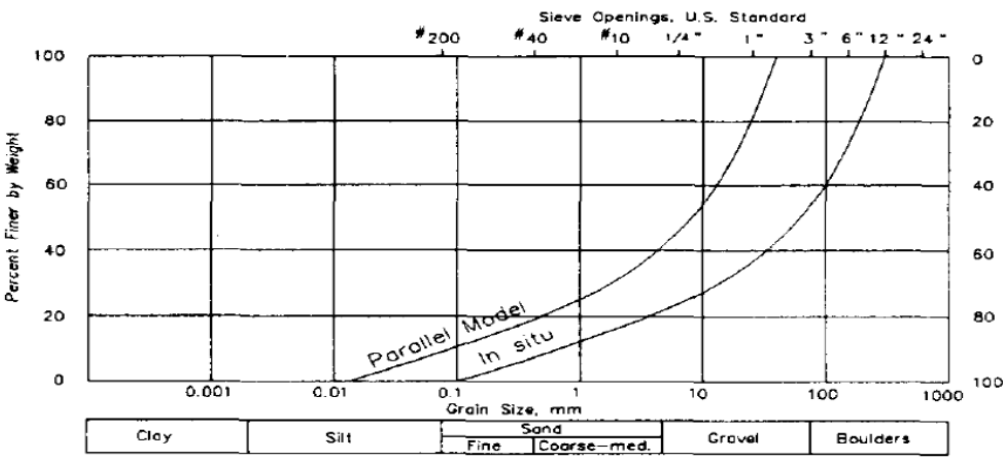

Figure 1: Parallel method illustrated with gradational analysis (Innacchione, 2000)

In the following parts, effective parameters for the determination of friction angle and shear strength have been described.

1. Parameters effecting shear strength of rockfill materials

1.1. Normal and Confining Pressure

Stress level affects the behavior of the rockfill material. Several authors have stated that the shear strength curve for rockfill is nonlinear, particularly at low confining pressures (triaxial: Marachi et al, 1969, Leps, 1970, and Indraratna et al.,1993). Therefore, in literature it is mentioned that a non-linear relationship should be applied for defining the failure envelope of this material. The increase of the normal stress reduces the peak friction angle (in decreasing rates) and the dilation angle. The rate of decrease diminishes as the normal stress becomes greater. This behavior can be explained as at very low confining stresses, the rockfill particles are relatively free to move with respect to each other and dilatancy effect can cause a significant increase in internal friction angle (Indraratna, 1994). The angle of dilation controls an amount of plastic volumetric strain developed during plastic shearing and is assumed constant during plastic yielding. As the confining stress increases, dilatancy effects gradually disappear due to particle crushing, causing a notable reduction of internal friction angle. This curved strength envelope of rockfill has a large impact on the stability analysis of rockfill dam due to the fact that a lower safety factor will be produced for the shallow slip surface when using constant friction angle (Indraratna, 1994; Barton and Kjaernsli, 1981).

The comparison of the materials' gradations before and after the tests shows that particle breakage occurs during the tests and the breakage amounts increases with increasing the normal stress. A number of correlations have been suggested to estimate the behavior of this material as well. Marachi et al (1969) carried out large scale triaxial tests on highly angular argillite, crushed basalt and rounded amphibolite and found that Ø does not appear to decrease significantly beyond $\sigma_n = 4.5$MPa. It should be noted that they did not perform tests beyond a confining pressure of 4.5MPa. Indraratna and his co-authors (Indraratna et al., 1993, 1998, Indraratna, 1994) performed tests on greywacke rockfill and basalt ballast. They found that the shear strength of the failure envelope was highly curved for confining stresses of less than 500kPa. Indraratna stated that the shear strength could be approximated by a linear Mohr-Coulomb criterion at stresses higher than 1.5MPa (as compared to the Marachi value of 4.5MPa above). Moreover, the comparison of the results of these tests with the results of the triaxial tests on the same material showed that the shear strength and peak friction angle from the direct shear tests were higher than those of the triaxial tests (Asadzadeh, 2009 and Lee et al 2009).

1.2. Water content and compaction

The water content, as the particles origin, has a double consequence. Initially, the increase of water content will affect the surface of particles where the condensation of water occurs. By affecting the surface of particles, it directly affects the inter-particle friction angle and in consequence a reduction in the shear strength can be obtained. The second consequence is related to the condensation of water in the particles micro-cracks, which influences the particles strength and facilitates the crushing. A trend was observed in the saturated specimens; however, wetting reduced the strength. The shear strength, peak friction angle, dilation angle, and particle breakage of the saturated specimens were less than those of the dry specimens. Performing similar tests in the dry-saturated tests shows that the strength parameters are less, but the particle breakage is more than those of the saturated tests. In these tests, also, saturation induced sudden settlement and shear stress reduction (Varadarajan et al 2006; Marsal, 1973).

1.3. Effect of Gradation

A number of researchers investigated the gradation effect on the shear strength by varying the coefficient of the uniformity (C_u) of rockfills. Marachi et al (1969) stated that a better graded rockfill, has a larger friction angle compared to uniform rockfill due to a better interlocking and less particle breakage in the former, the less breakage arises from the fact that in a well graded rockfill there are more inter-particle contacts and the load per contact is thus less than in a uniform rockfill. The impact of type of grading on the friction angle is about 2 to 3 degrees (Ghanbari et al., 2008).

1.4. Uniformity Coefficient

Generally, it could be expected that a poorly-graded rockfill (low uniformity coefficient, c_u), would have a higher strength than a well-graded rockfill assuming a constant void ratio for both. A well-graded material would be more likely to reduce the amount of dilation required due to the 'gaps' in the gravel matrix being filled with smaller particles. However, Marachi et al (1969) claim that if both rockfills were compacted to their maximum density then the well graded material could be expected to be stronger as it would have a greater density.

1.5. Maximum Particle Size

There is no common agreement on the effect of particle size on shear strength after evaluating the literature on this topic. Different views are presented with some indicating that the shear strength decreases with increasing particle size (Marachi et al., 1972; Marsal, 1973), while some have opposite views (Anagnosti & Popovic, 1982) or no effect at all (Charles & Watts, 1980). Some researchers have indicated that an increase in the particle size increases the load per particle, and hence crushing begins at a smaller confining stress, and causes a reduction in the friction angle; Barton (1981) showed that for materials compacted to the same density with geometrically similar grading, the smaller the elements are, the higher the friction angle of the material is. No effect at all has been observed by Charles & Watts, (1980). Marsal (1976) reports two triaxial tests each on rockfill-silt and rockfill-sand mixtures and compares these to a test on rockfill only. The clean rockfill and 10% sand-rockfill mixtures had Ø of 34.1° while the 30% sand-rockfill had a Ø of 39°. He attributes the difference to the lower initial void ratio in the 30% sand-rockfill mixture. The 10% silt-rockfill mixture showed a decrease in Ø to 28.8° while the 30% silt-rockfill mixture had the strength properties of the silt.

1.6. Influence of particles origin and shape

The nature of particles, such as shape and roughness have been studied by several authors (Marsal 1972, Marachi et al 1968). The particles origin concerns not only the mineralogic characteristics but also the extraction conditions, e.g., materials quarried from a mine, extracted by explosives, or extracted by backhoe, such as alluvial materials. The origin of a given material has a double mannered influence. First, the conditions of the particles surface affect the friction angle between particles, and second, the elastic and strength properties are dependent of the mineral characteristics. The mechanical characteristics of particles are then associated with the mechanical behavior of an equivalent continuum as a rockfill sample. Most researchers have focused on high quality rockfills. Kohgo et al (2007) supposed that rockfills with water absorption more than 10% are low quality materials and less than 3% is high quality material. Varadarajan et al (2006) showed that the angles of shearing resistance for quarried rockfill materials are higher than those for alluvial rockfill materials with comparable unconfined compressible strength of rockfill particles. Also, this angle for alluvial rockfill increases with the maximum particle size though the behavior of quarried rockfill material is the opposite. Nevertheless, this angle increases with the increase in unconfined compressive strength of alluvial rockfill particles. When breakage or crushing of particles happens, the grain-size distribution curve changes. In consequence the gradation curve measured at different stages of a test can reveal information about the amount of material crushed during the test. Nowadays, several constitutive models developed mainly on plasticity theory have incorporated the effect of particles' breakage, e.g., Salim and Indraratna (2004) and Kohgo et al. (2007). Kohgo's model is based on oedometric and triaxial tests conducted on two types of material (volcanic tuff and Andesite) tested both in dry and saturated state (Kohgo et al., 2007). He mentioned that breakage loads for particles of Tuff are strongly affected by the water content conditions but this effect for Andesite is small which may be due to difference in breakage characteristics of particles.

An angular rockfill may allow for stress concentrations that cause breakage of the particles at high confining pressures reducing dilation and leading to a lower overall rockfill strength than the rounded particles with less stress concentrations. The influence of grains' shape is an important factor for compacity, frictional and crushing characteristics. For frictional characteristics, the effect of grain's shape has been studied by Frossard (1979) who concluded that inter-particle friction angle seems to increase with angularity and that sphericity of particles has a notable effect on volumetric strains. As for compacity (i.e., the volume fraction that is filled), because during compaction the longer angular particles are more difficult to put in a dense arrangement than rounded regular particles. During loading stages, the flaws act as stress concentrators and will break easier than the rest of the particle. This will represent a higher deformability of the material. Due to the presence of flaws in angular particles and their breakage during loading, the angular materials can generate more finer particles than the non-angular materials. Some experimental results reported by Varadarajan et al. (2003) with alluvial (rounded) and quarried (angular) materials show strong differences between the behavior of both materials concerning shear resistance and deformation response. From discrete element analysis Nouguier-Lehon and Frossard (2005) showed that the angular particles dissipate less energy by rolling than rounded particles. This is explained by the restriction of rotations due to face to face contacts.

1.7. Density

It is generally accepted that the shear strength of rockfill increases with a higher relative density (Leps, 1970; Marsal, 1973). The effect of relative density on the friction angle can be explained by the phenomenon of interlocking the denser the rockfill; the greater the interlocking, a the greater the value of friction angle. The shape of the failure envelope is also affected by this factor. The dense rockfill specimens show a marked curvature on the stress -strain curve, with a distinct drop in the friction angle while the loose rockfill specimens shows minimal curvature and drop in friction because the loose material requires less dilation as particle have more freedom to move or rotate during shearing. The two curves tend to merge at very high confining pressures.

1.8. Influence of grain breakage

Factors like the size, shape and gradation of the particle are hardly analytically linked to the mechanical behavior of materials. Therefore, their association is made empirically, as the work of Barton and Kjaernsli (1981) who proposed as expression linking particle's size, shape and resistance to an equivalent friction angle of the media. The association made by Barton and Kjaernsli goes directly from particle's size and shape to the mechanical behavior in terms of friction angle. The approach taken here is relatively different. It is believed that factors such as particle's size, shape and gradation directly affect the breakage of particles, and then, breakage of particles affects the mechanical behavior of the rockfill materials. A detailed analysis of the influence of grain breakage on mechanical behavior of granular materials is the main subject of the next chapter. Table 1 presents a schematic correlation of the influence of different factors on breakage.

Table 1: Summary of factors affecting friction angle (Douglas, 2002).

Parameter	Effect on ϕ while increasing parameter	Comments
Effective normal stress (σ_n)	decrease	With high σ_n, ϕ is decreasing rapidly
Uniaxial compressive strength of rock	increase	More dilatancy, higher shear strength
Density	increase	More dilatancy, higher shear strength
Particle Size (D_{50})	decrease	
Ratio D_{max} /D_{50}	increase	
Angularity	increase	

2. Studies conducted by Direct Shear Test (DST)

Several investigators have tested shear resistance of rockfill using direct shear tests. Yamaguchi (2010) performed a shear box test on rockfill materials. In the test given under saturated conditions, the specimen was placed in a tank, fully immersed in water, as shown in Figure 1. He concluded that the large-scale box shear test can produce shear strength at a level similar to that of the large-scale triaxial compression test under the same normal stress (confining pressure), regardless of material type and whether the specimen is saturated or unsaturated, and can evaluate shear strength under a confining pressure lower than 49kPa, which is considered to be the verification limit of the large-scale compaction test.

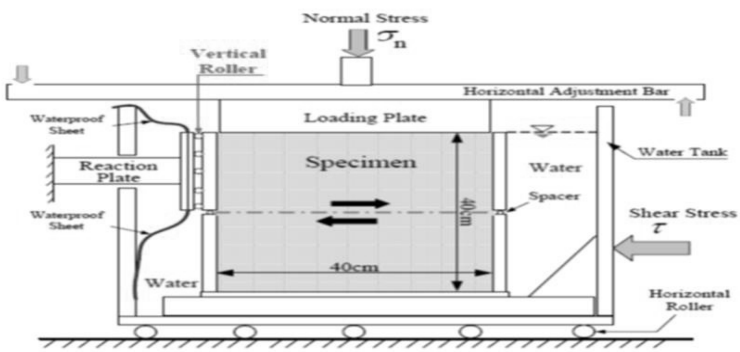

Figure 1: Schematic view of large scale shear box equipment (Yamaguchi, 2010).

Van der Linden, M. (2010) performed a shear test with medium scale box (Figure 2). In his tests, the density dependence of the rockfill is observed. Also, using Mohr- Coulomb's criterion, the obtained friction angles are in the range of 69° – 77° according to the test conditions, this would normally be around 50° (Indaratna, 1994) (Lee D. S., Kim, Oh, & Jeong, 2008). Lee et al (2009) mentioned that the obtained friction angles in his tests range from 39 to 49 degrees according to test conditions, with an average of 43.6^0. The larger values occur with greater density, smaller particle size, and air-dried samples, as recorded in previous studies based on large triaxial tests. Van der Linden justified that these values were due to wide range caused by the small range of normal stress applied and the few number of tests conducted. An increase in friction angle with an increase in density was seen. Dependency of the particle size on the friction angle is not clearly observed, due to the fact that there were only different fractions tested.

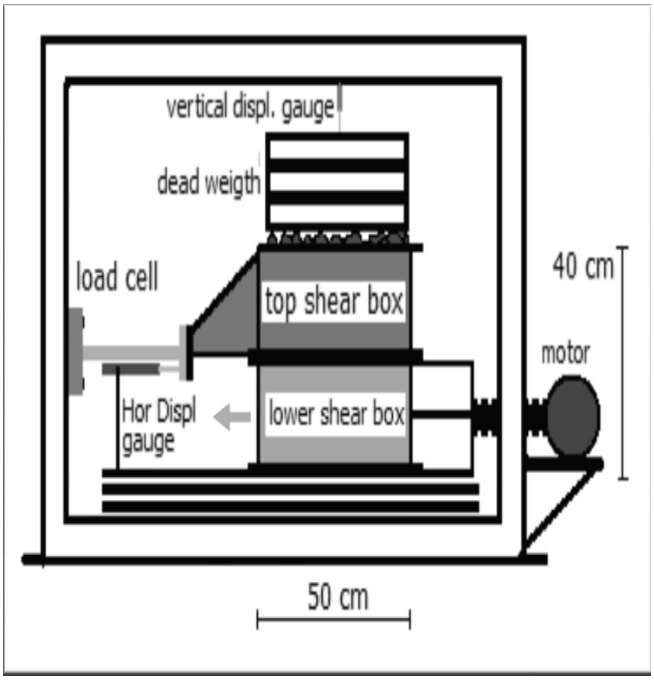

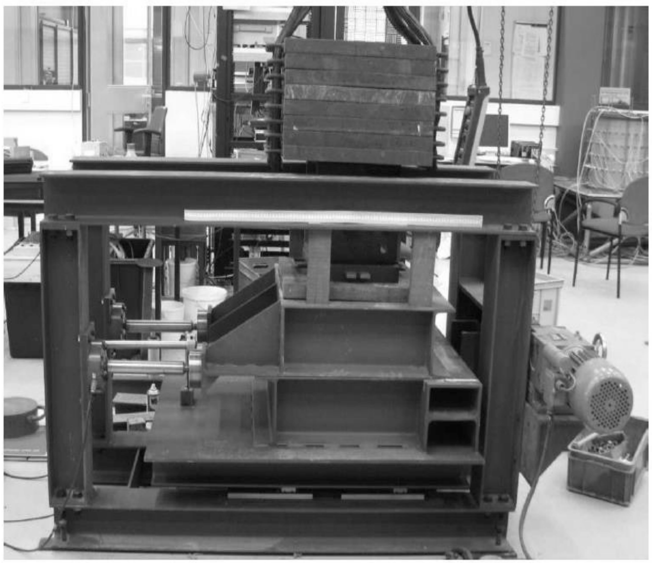

Figure 3: The direct shear box used, the orange arrow indicates the direction of shearing (Van der linden 2010).

Specimen size or scale effects were studied as early as 1936. Parsons presented test results for crushed quartz and for Ottawa uniform sand which showed that larger shear boxes produced lower values of friction angle (Moayed, 2012). Tests were done with very small, normal stresses to obtain the failure envelopes (0.015 to 0.1 kg/cm^2 or 1.5 to 9.8 kPa) that such low, normal stresses in conventional direct shear machines would be unlikely. Palmeira and Milligan's (1989) test results using three different size shear boxes showed shear zone thickness at the mid-height of sample was significantly affected by the scale factor (Moayed, 2012). The term "shear zone" means the small layer that is involved in the shearing process and the area where mechanism of localization occurs and this zone consists of many shear bands propagate from the edges of the shear box. Cerato and Luteneger (2006) performed DST using three different sizes of boxes (60 x 60 mm; 101.6 x 101.6 mm, and; 304.8 x 304.8 mm). In their study, they reported decrease in the friction angles with an increase of the shear box. They also studied the scale ratio of the specimen: height to diameter ratio (H/D) and width to maximum particle size ratio (W/D_{max}). They reported an increase of the friction angle with a decrease of the H/D ratio. Moreover, in literature it is often mentioned that square boxes are being used more frequently than circular boxes because circular boxes generate more problems during testing since the displacement sensors have to be placed more carefully (Ramírez Oyanguren et al, 2008).

Nakao and Fityus (2009) performed several large scale direct shear tests to study the factors that have an effect on the measured effective internal friction angle and to examine the effects of factors such as applied normal stress and shearing rate. Besides, to examine what effect the scale of the test has on the measured effective friction angle. The dimension of used shear box was 300 mm × 300 mm ×190 mm. Before testing commenced, the bulk sample was screened to remove all particles greater than 19 mm (about 10 % of the raw sample). The shearing rates were carried out at 7.06, 0.63, and 0.05 mm/min.

They concluded that shearing rate of around 7 mm/min is too fast to ensure fully drained (and hence maximum effective friction) behavior to be determined for the tested material using the large shear box. A shearing rate of around ten times slower would seem to give significantly higher effective friction angle values, but 100 times slower will give similar or even slightly reduced values. The results obtained here demonstrate that small shear box tests are no substitute for large shear box tests, and that downsizing the grading and the size of the sample tested will cause the effective friction angle to be under-estimated by as much as 4°. Moreover, Nakao and Fityus mentioned that shortcuts including testing a sample of reduced size in a small box, shearing the sample too quickly, and testing the same sample more than once in the testing of coarse granular materials will lead to significant differences in the measured results, that in most cases, are more conservative than the results obtained by adhering to the correct procedure.

REFERENCES

[1] Anagnosti, P. & Popovic, M., 1982. Evaluation of shear strength for coarse-grained granular materials. In Fouteenth Congres on Large Dams. Rio de Janeiro, 1982. ICOLD.

[2] Asadzadeh M., "Direct shear testing on rockfill material". Arabian journal for science and engineering, vol 34, number 2B October, pp 379-396, (2009).

[3] ASTM D3080/D3080M – 11, "Direct Shear Test of Soils Under Consolidated Drained Conditions", (2004).

[4] Bagherzadeh A., "Numerical and experimental direct shear tests for coarse grained soils". Journal of Particuology, vol. 7, no. 1, pp. 83-91, (2009).

[5] Barton, N., and Kjanernsli., "Shear strength of rockfill". Journal of the Geotechnical Engineering Division, Vol. 107, No. 7, July 1981, pp. 873-891, (1981).

[6] Barton, N.R. "Review of a new shear strength criterion for rock joints". *Engineering Geology*, vol. 7, issue 4, pp. 287-332, (1973).

[7] Barton, N.R. "The shear strength of rock and rock joints". International Journal for Rock Mechanics, Mining Sciences and Geomechanical Abstracts, vol.13, No.9, pp. 255-279, (1976).

[8] Cerato, A.B. & Lutenegger, A.J.," Specimen size and scale effects of direct shear box tests of sands". Geotechnical Testing Journal, 29(6), pp.1-10, (2006).

[9] Cetin H. et al., "Settlement and slaking problems in the world's fourth largest rock-fill dam, the Ataturk Dam in Turkey". Engineering Geology, vol.56. pp. 225–242, (2000).

[10] Charles J.A., "The engineering behaviour of fill materials: the use, misuse and disuse of case histories". Geotechnique 58, No. 7, 541–570, (2008).

[11] Charles, J.A. & Watts, S.K. The influence of confining pressure on the shear strength of compacted rockfill, Geotechnique, 30(4), pp.353-67, (1980).

[12] Frossard E. et al. "Rockfill shear strength evaluation: a rational method based on size effects". Ge´otechnique 62, No. 5, 415–427, (2012).

[13] Ghanbari A. et al., "An Experimental Study on the Behavior of Rockfill Materials Using Large Scale Tests". Electronic Journal of Geotechnical Engineering, Vol. 13, Bundle G, (2008).

[14] Hamidi A., "Impact of gradation on the shear strength-dilation behavior of well graded sand-gravel mixtures". Scientia Iranica, Volume 19, Issue 3, June 2012, pp. 393–402, (2012).

[15] Innachione A.T, Vallejo L.E., "Shear strength evaluation of clay- rock mixtures". Book Chapter TA - Slope Stability 2000, (2000).

[16] Indraratna, B., "The effect of normal stress -friction angle relationship on the stability analysis of a rockfill dam". Geotechnical and Geological Engineering, 12, pp.113- 21, (1994).

[17] Indraratna, B., Ionescu, D. and Christie, H.D. "Shear behaviour of railway ballast based on large-scale triaxial tests".Journal of Geotechnical and Geoenvironmental Engineering, vol.124 (5), pp. 439-449, (1998).

[18] Indraratna, B., Wijewardena, L.S.S. and Balasubramaniam, A.S. "Large-scale triaxial testing of greywacke rockfill". *Geotechnique*, 43 (1), pp. 37-51, (1993).

[19] Jewell, R. A. and Wroth, C. P., "Direct Shear Tests on Reinforced Sand". Geotechnique, Vol. 37, No. 1, pp. 53–68, (1987).

[20] Kohgo, Y., I. Asano, and Y. Hayashida. " Mechanical properties of unsatured low quality rockfills. Soils and Foundations 47(5), 947–959, (2007).

[21] Lee, D.S., Kim, K.Y., Oh, G.D. & Jeong, S.S, "Shear characteristics of coarse aggregates sourced from quarries". International Journal of Rock Mechanics & Mining Sciences, 46, pp.210-18, (2008).

[22] Leps, T."Review of shearing strength of rockfill". Journal of the Soils Mechanics and Foundations Division. ASCE 96(SM4), 1159–1170, (1970).

[23] Marachi, D.N., Chan, C.K. & Seed, B.H., "Evaluation of properties of rockfill materials". Journal of the Soil Mechanics and Foundations Division, 98(SM1), pp.95-114, (1972).

[24] Marsal, R.J. “Large scale testing of rockfill materials”. Journal of the Soil Mechanics and Foundations Division Proceedings of the American Society of Civil Engineers, vol.93 (SM2), pp. 27-43, (1976).

[25] Marsal, R.J. “Mechanical properties of rockfill”. In Embankment Dam Engineering Journal. Willey & Sons, N.Y., pp. 109-201, (1973).

[26] Moayed R.Z, Alizadeh A., “Effects of shear box size on the strength for different type of silty sands in direct shear tests”. 5th Asia-Pacific Conference on Unsaturated Soils 2012, Volume 1, 2012, pp. 248-254, (2012).

[27] Nakao, T., Fityus, S., “Direct Shear Testing of a Marginal Material Using a Large Shear Box”. Geotechnical Testing Journal, Vol. 31, No. 5, (2008).

[28] Palmeira, E.M. and Milligan, G.W.E.,” Scale effects in direct shear tests on sand”. In Proceedings from the 12th. International Conference on Soil Mechanics and Foundation Engineering, Balkema, Rotterdam, 1, pp. 739-742, (1989).

[29] Ramírez Oyanguren, et al, “Stability analysis of Llerin Rockfill Dam: An in situ direct shear test”. Engineering Geology No.100, pp.120–130. (2008).

[30] Salim, W. and B. Indraratna. ” A new elastoplastic constitutive model for coarse granular aggregates incorporating particle breakage. Canadian Geotechnical Journal 41(4), 657–671, (2004).

[31] Van der Linden, M., “Determine shear strength of Bremanger aggregate at low normal stress using medium size direct shear box tests”. BSc. Thesis. TU Delft, (2010).

[32] Varadarajan A., “Testing and Modeling Two Rockfill Materials”. Journal of Geotechnical and Geoenvironmental engineering, vol 129, issue 3, pp. 206–218, (2003).

[33] Varadarajan A. et.al., “The role of nature of particles on the behavior of rockfill materials**”**. Journal of soils and foundations, vol 46, issue 5, pp. 569-584, (2006).

[34] Yamaguchi,Y, “Strength evaluation of rockfill materials considering confining pressure dependency”. The 1st International Symposium on Rockfill Dams, (p.10). Minamihara, (2010).

INTERNATIONAL JOURNAL OF ELECTRONICS, MECHANICAL AND MECHATRONICS ENGINEERING

Submission Instructions

The scope of International Journal of Electronics, Mechanical and Mechatronics Engineering (IJEMME) covers the novel scientific papers about Electronics, Image Processing, Information Theory, Electrical Systems, Power Electronics, Control Theory, Embedded Systems, Robotics, Motion Control, Stochastic Modeling, System Design, Multidisciplinary Engineering, Computer Engineering, Optical Engineering, Design Optimization, Material Science, Metamaterials, Heat and Mass Transfer, Kinematics, Dynamics, Thermo-Dynamics, Energy and Applications, Renewable Energy, Environmental Impacts, Structural Analysis, Fluid Dynamics and related topics of the above subjects.

IJEMME is an international journal published four times a year (January, April, July and October). Manuscripts reporting on original theoretical and/or experimental work and tutorial expositions of permanent reference value are welcome. IJEMME Editorial Board is authorized to accept/reject the manuscripts based on the evaluation of international experts. The papers should be written in English.

The manuscript should be sent in electronic submission via IJEMME paper submission system of web address (www.aydin.edu.tr/ijemme)

Submission instructions of manuscripts.

Page Design: Text body area is (195mm x 275mm). 30 mm margin from top, 20 mm from down and 25 mm margin should be left on right/left sides.

Title should be in 16 pt. bold, capital letters with Times New Roman font in Microsoft Word format. Authors' names, affiliations, e-mail addresses should follow the title after double line spacing with authors' names and surnames in lower case except first letters in 14 pt, the rest is 10 pt. italic.

Abstract should not exceed 200 words with the word "Abstract" in 10 pt. italic, bold, abstract text in 9 pt. italic, all in Times New Roman font in Microsoft Word format.

Key Words not exceeding 5 should be in bold.

Document Character: Subtitles should be in 10 pt. bold, capital letters and text body 10 pt. both with Times New Roman font in Microsoft Word format. The manuscripts should be written on a single column, be double spaced with single line spacing between paragraphs. The subtitle of the first section should start after a single space following the keywords, the other subtitles also with a single line space following the text, there should also be single line spacing between the previous text and the subtitle.

Conclusion: section should have a title written in 1o pt. bold, capital letters and the text in 10 pt. all in Times New Roman font in Microsoft Word format.

Reference numbers should be given in brackets as illustrated below:

Referencing books:
[1] Özsu M., T, Valduriez, P., *Principles of Distributed Database Systems*, Prentice Hall, New Jersey, 128-136,1991.

Referencing papers:
[2] G. Altay, O. N., Ucan, "Heuristic Construction of High-Rate Linear Block Codes," *International Journal of Electronics and Communications (AEU),* vol. 60, pp.663-666, 2006.

Page number is to be placed at the top left corner of each page with pencil.
Length of the Manuscript should not exceed 20 pages excluding Figures and Tables.

INSTRUCTIONS ABOUT THE ACCEPTED MANUSCRIPTS:

Page Design: Text body area is (195mm x 275mm). 30 mm margin from top, 20 mm from down and 25 mm margins should be left on right/left sides.

Title should be in 16 pt. bold, capital letters with Times New Roman font in Microsoft Word format. Authors' names, affiliations, e-mail addresses should follow the title after double line spacing with authors' names in lower case and surnames in capital letter in 14 pt. the rest in 10 pt. in the same format.

Abstract should not exceed 200 words with the word "Abstract" in 12 pt. italic, bold, abstract text in 9 pt. italic, all in Times New Roman font in Microsoft Word format.

Key Words not exceeding 5 should be in 9 pt. bold.

Document Character: Subtitles should be in 10 pt. bold, capital letters and text body 10 pt. both with Times New Roman font in Microsoft Word format. The manuscripts should be written on two columns, be single spaced with single line spacing between paragraphs. The subtitle of the first section should start after a single space following the keywords, the other subtitles also with a single line space following the text, there should also be single line spacing between the previous text and the subtitle.

Sections: Formulas should be numbered sequentially. Referring to formulas should be as Eqn (.). Figures and Tables should be placed into the text body and captions for both should be 10 pt. Table numbers and captions should be placed before the Table. If necessary, both columns may be used for large Figures and Tables.

Conclusion section should have a title written in 12 pt. bold, capital letters and the text in 10 pt. all in Times New Roman font in Microsoft Word format. Conclusion should not be a version of the Abstract.

Reference numbers should be given in brackets as illustrated below:

Referencing books:
[1] Özsu M., T, Valduriez, P., *Principles of Distributed Database Systems*, Prentice Hall, New Jersey, 128-136,1991.

Referencing papers:

[2] G. Altay, O. N., Ucan, "Heuristic Construction of High-Rate Linear Block Codes*," International Journal of Electronics and Communications (AEU),* vol. 60, pp.663-666, 2006.

Short Biography of the authors should follow references after a single line space, names in 9 pt. surnames in 9 pt. and the text in 9 pt. The text should not exceed 100 words.

CORRESPONDENCE ADDRESS:

Editor in Chief
Prof. Dr. Hasan Alpay HEPERKAN
Istanbul Aydın University, Faculty of Engineering
Mechanical Engineering Department
Florya Yerleskesi, Inonu Caddesi, No.38, Kucukcekmece, Istanbul, Turkey
Fax: +90 212 425 57 59 - Tel: +90 212 425 61 51 / 22001
E-mail: hasanheperkan@aydin.edu.tr

Prepared by
Instructer:Saeid KARAMZADEH
Engineering Faculty
Electrical and Electronics Eng. Dept.
Inonu Caddesi, No.38, Florya, Istanbul, TURKEY
E-mail: saeidkaramzadeh@aydin.edu.tr

Published by
Istanbul Aydın University
Graphic Design Department

KÜTÜPHANE VE BİLGİ MERKEZİMİZ 7/24 HİZMET VERİYOR

56.000
Basılı Kaynak

1.000.000
E-Kaynak

Engelsiz Kütüphane

Mobil Uygulamalar

24/7

- Kütüphane 7/24/365 gün hep açık
- 75.000 aylık kullanıcı
- Mimarlık ve Mühendislik Fakültesi için çizim salonları
- Kafeterya